European Journal of Radiology Open 8 (2021) 100387

Contents lists available at ScienceDirect

European Journal of Radiology Open

journal homepage: www.elsevier.com/locate/ejro

Original Research

Texture-based probability mapping for automatic scar assessment in late gadolinium-enhanced cardiovascular magnetic resonance images

Vidar Frøysa [a,*], Gøran J. Berg [b], Trygve Eftestøl [b], Leik Woie [b], Stein Ørn [a,b]

[a] Department of Cardiology, Stavanger University Hospital, Armauer Hansens vei 20, 4011, Stavanger, Norway
[b] Department of Electrical and Computer Science, University of Stavanger, P.O. box 8600, 4036 Stavanger, Norway

HIGHLIGHTS

- Texture based probability mapping can be used to evaluate myocardial scar size.
- The method can assess myocardial fibrosis independent of signal intensity.
- The TPM method shows strong correlations between scar size and left ventricular ejection fraction.

ARTICLE INFO

Keywords:
Cardiac magnetic resonance. Late gadolinium enhancement. Myocardial infarction. Machine learning. Left ventricular remodeling

ABSTRACT

Purpose: To evaluate a novel texture-based probability mapping (TPM) method for scar size estimation in LGE-CMRI.

Methods: This retrospective proof-of-concept study included chronic myocardial scars from 52 patients. The TPM was compared with three signal intensity-based methods: manual segmentation, full-width-half-maximum (FWHM), and 5-standard deviation (5-SD). TPM is generated using machine learning techniques, expressing the probability of scarring in pixels. The probability is derived by comparing the texture of the 3 × 3 pixel matrix surrounding each pixel with reference dictionaries from patients with established myocardial scars. The Sørensen-Dice coefficient was used to find the optimal TPM range. A non-parametric test was used to test the correlation between infarct size and remodeling parameters. Bland-Altman plots were performed to assess agreement among the methods.

Results: The study included 52 patients (76.9% male; median age 64.5 years (54, 72.5)). A TPM range of 0.328–1.0 was found to be the optimal probability interval to predict scar size compared to manual segmentation, median dice (25th and 75th percentiles)): 0.69(0.42–0.81). There was no significant difference in the scar size between TPM and 5-SD. However, both 5-SD and TPM yielded larger scar sizes compared with FWHM ($p < 0.001$ and $p = 0.002$). There were strong correlations between scar size measured by TPM, and left ventricular ejection fraction (LVEF, $r = -0.76$, $p < 0.001$), left ventricular end-diastolic volume index ($r = 0.73$, $p < 0.001$), and left ventricular end-systolic volume index ($r = 0.75$, $p < 0.001$).

Conclusion: The TPM method is comparable with current SI-based methods, both for the scar size assessment and the relationship with left ventricular remodeling when applied on LGE-CMRI.

1. Introduction

Following myocardial infarction (MI), the scar size estimation adds valuable information about left ventricular remodeling and prognosis [1]. Late gadolinium-enhanced cardiovascular magnetic resonance imaging (LGE-CMRI) has become the gold standard for assessing scar size following MI [2,3]. Current methods use pixel- and regional differences in signal intensity (SI) to assess scar size either by manual planimetry,

Abbreviations: CMR, Cardiac magnetic resonance; MI, Myocardial infarction; LGE, Late gadolinium enhancement; FWHM, Full-width-half-maximum; 5-SD, 5 standard deviation; LV, Left ventricle; TPM, Texture-based probability mapping; SI, Signal intensity.

* Corresponding author.
E-mail addresses: vidarf@gmail.com (V. Frøysa), goran.j.berg@uis.no (G.J. Berg), trygve.eftestol@uis.no (T. Eftestøl), leikw@online.no (L. Woie), drsteinorn@hotmail.com (S. Ørn).

https://doi.org/10.1016/j.ejro.2021.100387
Received 2 September 2021; Received in revised form 16 November 2021; Accepted 22 November 2021
Available online 3 December 2021

the n-standard deviation (SD) technique, or the full width half maximum (FWHM) technique [4]. In manual planimetry, the demarcation between scarred and non-scarred myocardium is done by visual assessment [4]. The n-SD method uses the standard deviation of SI-values in non-scarred myocardium to define the scarred myocardium (most commonly 5-SD) [4]. In the FWHM method, the scar is defined as pixels with a SI of more than 50% of the maximal SI of any pixel within the scar. Contemporary SI-based methods have several limitations [5,6]. These methods require that regions of interest (ROI) are defined on each slice. Outlining and verification are both time-consuming and vulnerable to imprecisions and inter-observer variability. Furthermore, in slices with little contrast in SI between scarred and non-scarred myocardium, it may be hard to define the true ROI, and the n-SD and the FWHM may over-or underestimate the size of the LGE depending upon the range of SI of the pixels [7]. It would therefore be beneficial to develop methods that overcome the challenges with SI as mentioned above.

The analysis of image texture is one of the main pillars of radiomics [8]. Image texture is not bound by a strict definition but can be described as the arrangement of gray-level pixel patterns providing image properties such as coarseness, randomness, and smoothness [9]. Data characterization algorithms of textural features can be used to study image properties that cannot be visualized using standard SI-based methods [5, 10]. In this study, we evaluate the potential use of a semi-automatic texture-based method for the assessment of myocardial scar size in LGE-CMRI. The texture-based probability mapping (TPM) method is generated by a machine learning technique using reference dictionaries to calculate the scar size in new LGE images [11]. The TPM method calculates each pixel's probability of being scar tissue and is not dependent upon regional differences in SI. The TPM provides each pixel with a probability ranging between 0 and 1. However, the probability range most closely resembling conventional scar segmentation has not been found. Therefore, the present study first determined the TPM probability range most closely related to manual scar segmentation. Then the TPM based scar size was compared with the scar size found by contemporary SI based methods (FWHM and 5-SD). Finally, the pathophysiological link between scar size and left ventricular remodeling was assessed for all four methods for scar size measurement.

Due to limitations with SI-based methods already mentioned and the potential of using a texture-based approach, we conducted this study to explore the TPM method`s properties in myocardial scar assessment.

The hypothesis of our study was that TPM applied on LGE-CMRI will be able to recognize chronic myocardial infarction when applying the appropriate probability threshold.

Thus, the purpose of our proof-of-concept study was to assess the diagnostic potential of the TPM as a texture-based method without the use of SI.

2. Methods

2.1. Patient population

This single-center retrospective analysis was based upon CMR images from 54 patients with chronic ischemic scars (> 1 year old) (Table 1). The analysis was approved by The Regional Ethics Committee (REK Vest: 3.2005.1312). All included patients signed an informed consent.

We used CMR images from our study database of chronic myocardial scars obtained in the period of 2004 – 2006 [1,12]. The patients had no other known cardial diseases, and there were no sign of microvascular obstruction.

The TPM method was evaluated on LGE-CMRI. Cine CMR images were used to assess left ventricular remodeling. All CMR examinations, both those previously used to generate the dictionary and the images of the patients used in the current study, were acquired using the same hardware, image acquisition protocols, contrast agent, and software.

Table 1
Baseline characteristics.

Variables (n = 52)	
Age (years)	64.5 (54, 72.5)
Male/female	40/12
Number of coronary vessel(s) involved	
1 vessel	38 (73%)
2 vessels	3 (6%)
3 vessels	11 (21%)
Heart failure treatment	
ß-Blockers	36 (69%)
ACEi/AT2 blockers	46 (89%)
Aldosterone-antagonists	13 (25%)
CMR findings	
LVEF (%)	44 (32,55)
LVEDVi (ml/m^2)	106 (87, 139)
LVESVi (ml/m^2)	57 (39,93)

Data are expressed as absolute numbers, percent of total or median with 25th and 75th percentiles. LVEF left ventricular ejection fraction, LVEDVi left ventricular end-diastolic volume index, LVESVi left ventricular end-systolic volume index, ACEi angiotensin-converting enzyme inhibitor, AT2 angiotensin type 2 receptor blocker, CMR cardiovascular magnetic resonance.

2.2. The texture-based probability mapping (TPM) method

The TPM method uses dictionaries and machine learning (ml) techniques (quadratic discriminant analysis) to generate texture-based probability maps [11]. Even though the dictionary is based on a limited dataset, it's generated using cross-validation and an ml algorithm that is not sensitive to overtraining, and the results should therefore not be compromised. The calculation of the probability of scarring in each pixel is based upon the comparison of a 3 × 3 pixels matrix (patch) surrounding each pixel, with a dictionary constructed from 3 × 3 pixel matrices of LGE images in patients with established myocardial scars (Fig. 1) [11]. The method is based on the application of Bayes` theorem. For each slice, the posterior probability of that pixel being scar compared with healthy myocardium is estimated. The posterior probabilities are calculated using features from the myocardium and estimates of the two classes´ prior probabilities and class-specific

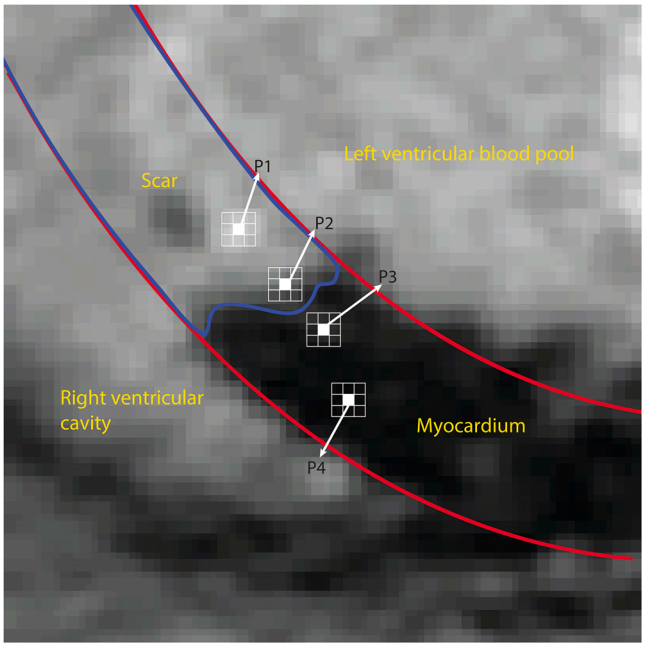

Fig. 1. Varieties of signal intensity of the matrices. Fig. 1 shows a LGE-MRI with a myocardial ischemic scar (bright pixels delineated by a blue line). P1: Core. P2: Border zone. P3-P4: Normal myocardium, but still, there is a variety in signal intensity. Fig. 2.

density functions of the features and validated from a labeled training set of features. The texture was defined as a repetitive pattern of primitives. One dictionary for non-scar myocardium (Dm) and one for scar tissue (Ds) were trained so that the patches can be reconstructed. Thus, each patch is reconstructed from linear combinations of texture primitives, both from Ds and Dm. The representation error is calculated for each reconstruction (Rm and Rs), and a textural feature is expressed as the ratio between these: Rp = Rm/(Rs+Rm). A high Rp means that the patch resembles scar tissue. A classifier was trained to distinguish scar tissue from normal tissue based on Rp. The classifier yields probability values for two categories, of which the one expressing the probability of scarred tissue defines the TPM. The TPM method requires that epicardial and endocardial contours are determined, but it does not require a separate ROI to identify scarred and non-scarred myocardium prior to the analysis. Each pixel is provided a color code indicating the probability (0−1) that the pixel represents scarred tissue. The probability map consists of all color-coded pixels from each slice (Fig. 2).

2.3. Image acquisition

Images were acquired on a 1.5-T Philips Intera R 8.3 (Philips Medical Systems, Best, The Netherlands). To assess left ventricular ejection fraction (LVEF), left ventricular end-diastolic volume index (LVEDVi), and left ventricular end-systolic volume index (LVESVi), we used a steady-state free precession sequence (balanced fast field echo) covering the entire left ventricle with a slice thickness of 8 mm and an interslice gaps of 2 mm. Images were acquired during breath-holding. Following functional assessment, LGE sequences were obtained 10–15 min after administering a 0.25 mmol/kg gadolinium-based contrast agent (Omniscan®, GE HealthCare technologies Norway AS, Nycoveien1, 0484 Oslo, Norway). We used an inversion-recovery-prepared T1-weighted gradient-echo (T1-GRE) sequence with TR 4.1 ms (range 4.0–4.2 ms) and TE 1.3 ms. The pixel size was $0.82 \times 0.82\ mm^2$, covering the whole ventricle with short-axis 10 mm thick slices without an interslice gap. The inversion time was individually adjusted, aiming to null the normal myocardial signal (typically 200–300 ms).

2.4. Processing of LGE images

The images were stored in Digital Imaging and Communications in Medicine (DICOM) format, with 512 × 512 pixels and a bit depth of 12. Because of anatomical and partial volume artefacts, we excluded the most apical cross-sectional images and the basal parts at the level of the left ventricle outflow tract. Median image slices per patient included in the analyses were 7 (IQR 1). The LGE-CMR images were analyzed using in-house-developed software programs written in MATLAB® (Natick, Massachusetts, USA). ViewForumTM (Philips Medical Systems, Best, The Netherlands) was used for the original assessment of LV volumes, analyzing the full short-axis dataset in a random blinded fashion, without the knowledge of infarct size. LV volumes were indexed for body surface area to compensate for the large range in body size.

The ICC values were recognized to be low at the start of the study, with interobserver ICC = 0.908 for myocard and 0.838 for scar. The scar, endo- and epicardial borders were therefore drawn in consensus by two cardiologists experienced in CMR (SØ, 20 years of experience, and LW, 10 years of experience)). The same contours were used for all methods. When assessing the presence for LGE, all projections were studied in detail. Enhancement had to be visual in three different axis views. The readers were blinded to earlier image examinations and medical history except that they had a history of acute MI.

The segmentations created in MATLAB were used to create probability maps (done by G.J.B), where high- and low- probabilities indicate scarred and normal tissue, respectively. A color figure was used to visualize the probability maps (Fig. 2). Shades from green to yellow and towards red show increasingly damaged myocardium, while blue indicates normal tissue. By adjusting the lower probability threshold, we could study different parts of the myocardium according to its scarring resemblance and find the optimal interval to fit manual demarcation, which is the most used method for assessing infarct size (done by G.J.B). This process was done by using the Sørensen-Dice coefficient[13,14], which measures similarities between sets by dividing twice the number of elements common to the two sets by the total number of elements. Cardiac segments (CS) were examined for the ranges 0.290–1.0, 0.291–1.0. 0.349–1.0 (60 values). We split the cohort (n = 52) into five groups: test1. test5, with 10 or 11 patients in each group. By leaving a different test group out at the time, we get five different training groups. The Dice coefficient was calculated for each slice. The performance was calculated by first calculating the median (dice) across the slices for each patient and then the median of these calculations. For each training set, the median dice coefficient was calculated for all ranges. The scar size of the TPM was compared with the two other semi-automatic methods: the 5-SD and the FWHM, using the probability range 0.328–1.

2.5. Statistical analysis

All statistical analyses were performed using SPSS for Windows, Rel. 26.0.0.1. Chicago: SPSS Inc., and MATLAB®. Continuous variables are expressed as mean ± standard deviation (SD) for normally distributed variables and medians with 25th and 75th percentiles for non-normally distributed variables. The Shapiro-Wilk test was used to assess normality. Spearman`s rho correlations coefficient was used to assess the relationship between the infarction size estimated by the different

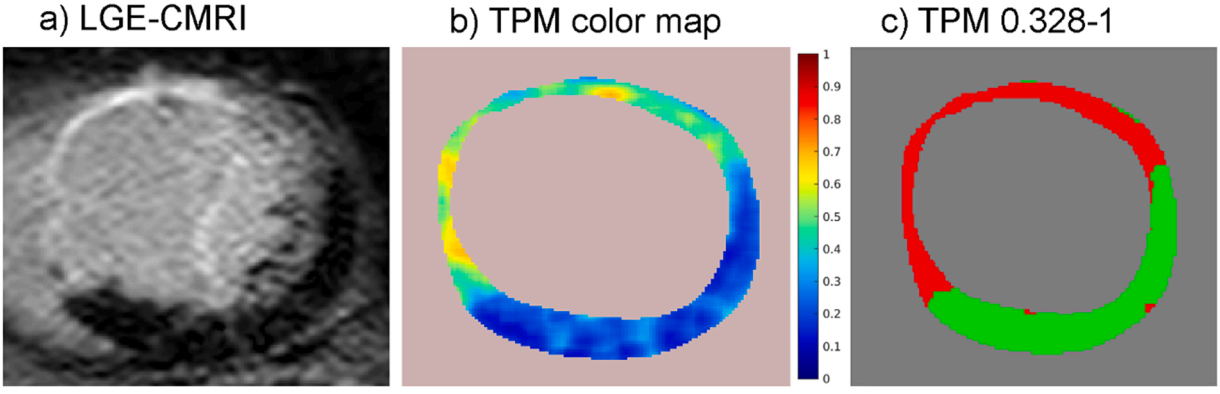

Fig. 2. Assessment by the TPM-method a) Original LGE-CMRI with Corresponding TPM color map (b). Shades of blue indicate normal myocardium, and green, yellow and orange indicate scarred myocardium with higher probability as the color gets more intense. We can appreciate the smooth transition between normal and scarred myocardium which is thought to make more sense physiologically compared with the crisp segmentation by the hand of the cardiologist. c) TPM with a cutoff threshold of 0.328. All pixels above that threshold are red, and pixels below are green.

methods and LV volumes and functions. Bland–Altman plots were used to assess agreement among the methods. All tests were two-sided, and $p < 0.05$ was considered statistically significant. The Sørensen-Dice coefficient was used to compare the manual segmentation to different lower thresholds of TPM.

3. Results

3.1. Baseline characteristics

The reference CMR images were obtained from 54 patients (78% male; median age 65 years (54, 74)) with chronic myocardial scars (>1 year). Images from two patients were excluded due to fold-over and motion artifacts. The baseline characteristics of the remaining 52 patients are provided in Table 1. No image had evidence of microvascular obstruction.

3.2. Pixel distribution and probability range

The pixel distribution of the probability intervals computed by the TPM of all 52 patients is presented in Fig. 3. The maximum achieved probability for any pixel was 0.75. When combining manual assessment of the infarct size and cross-validation, the optimal TPM-range for myocardial scarring was found with the probability range 0.328–1.0: Sørensen-Dice (median (25th and 75th percentiles)) 0.69(0.42–0.81), sensitivity 0.87 (0.61–0.91) and specificity 0.92 (0.85–0.96). Hence, all pixels with a higher probability than 0.328 were classified as scar and designated with the color red. Values below this probability threshold were designated green color (Figs. 2 and 4). The majority of pixels were located in the lower probability interval range, indicating that most pixels represent normal myocardium.

3.3. Comparing infarct size measurements and LV remodeling

Fig. 4 illustrates the difference between the four methods calculating infarct size. The FWHM generated the smallest infarct size estimates, while the 5-SD estimated the largest (Table 2). There was no significant difference in infarct size estimation between TPM and 5-SD. The TPM estimated larger infarctions compared with the FWHM ($p < 0.02$). There was also a significantly larger estimated infarct size using manual planimetry compared with FWHM ($p = 0.001$). We compared the scar size estimates by TPM with the manual, and the two semi-automatic method using Bland-Altman plots (Fig. 5). Fig. 5b shows an increasing difference between scar size estimated by TPM and FWHM with increasing scar size. To compare the different methods with the relationship of adverse response, the infarct size assessments of all methods were compared with parameters of left ventricular remodeling (LVESVi and LVEDVi) and function (LVEF). The TPM method demonstrated similar correlations with left ventricular remodeling compared with the three other methods (manual, FWHM, and 5-SD, Table 3).

4. Discussion

The present study suggests that the TPM method can be used to estimate infarct size, and is comparable with contemporary SI-based methods. Furthermore, the correlation between TPM based scar size and left ventricular remodeling indicates that the TPM based scar size is related to important pathophysiological mechanisms such as left ventricular remodeling. However, compared with the FWHM, the TPM generated a larger infarct size estimation and a less strong relation between infarct size and LV remodeling. This finding underscores that the TPM relates to other properties than those measured by FWHM.

When comparing the TPM method to manual segmentation, which still is the gold standard when done by an expert reader, Fig. 5a shows a positive bias, implying an overestimation of fibrosis. However, the present work is a proof-of-concept, and the potential complementary

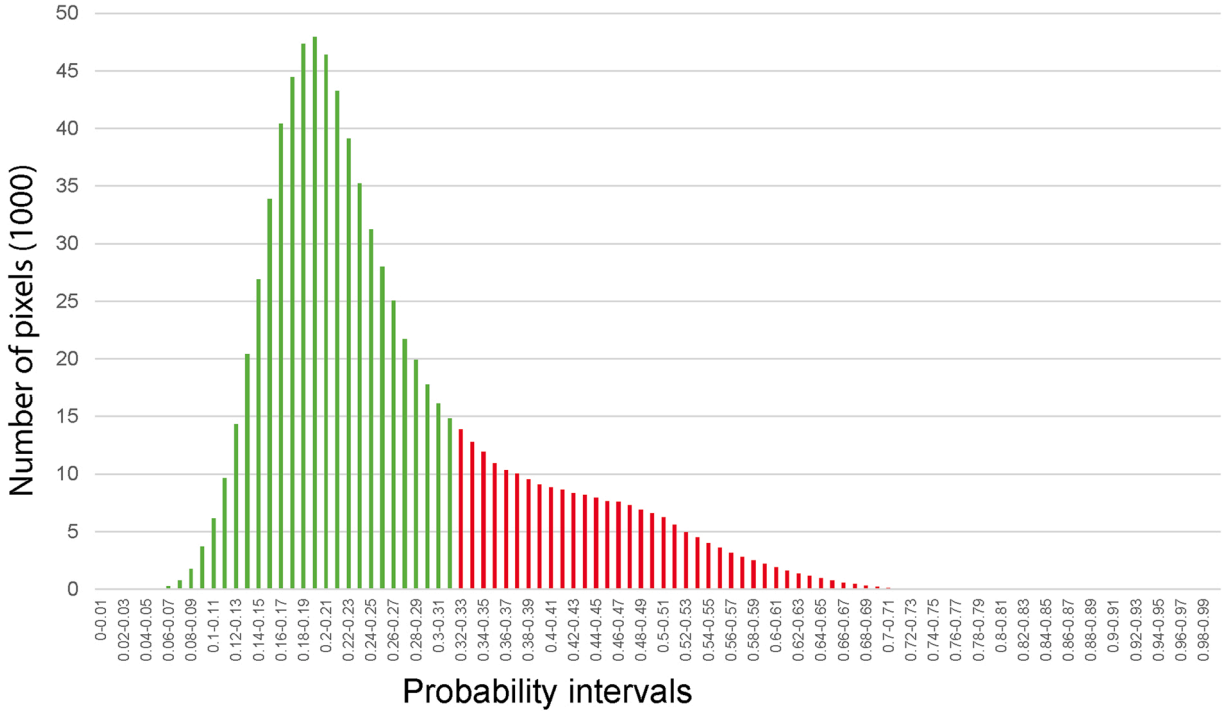

Fig. 3. Pixel distribution The figure displays how the probability distributes for all pixels of the 52 patients analyzed in the present study. Since the manual delineation is based on visual interpretation of SI, and the TPM is based on replicating this from texture information, the recognition accuracy and the probabilities will not reach higher than 0.75. The probability threshold between scarred and non-scarred pixels comparing the TPM method with the manual demarcation was found to be 0.328. Pixels with a probability value below this limit were defined as non-scar (green), whereas pixels with a probability value above this limit are considered to represent scarred tissue (red).

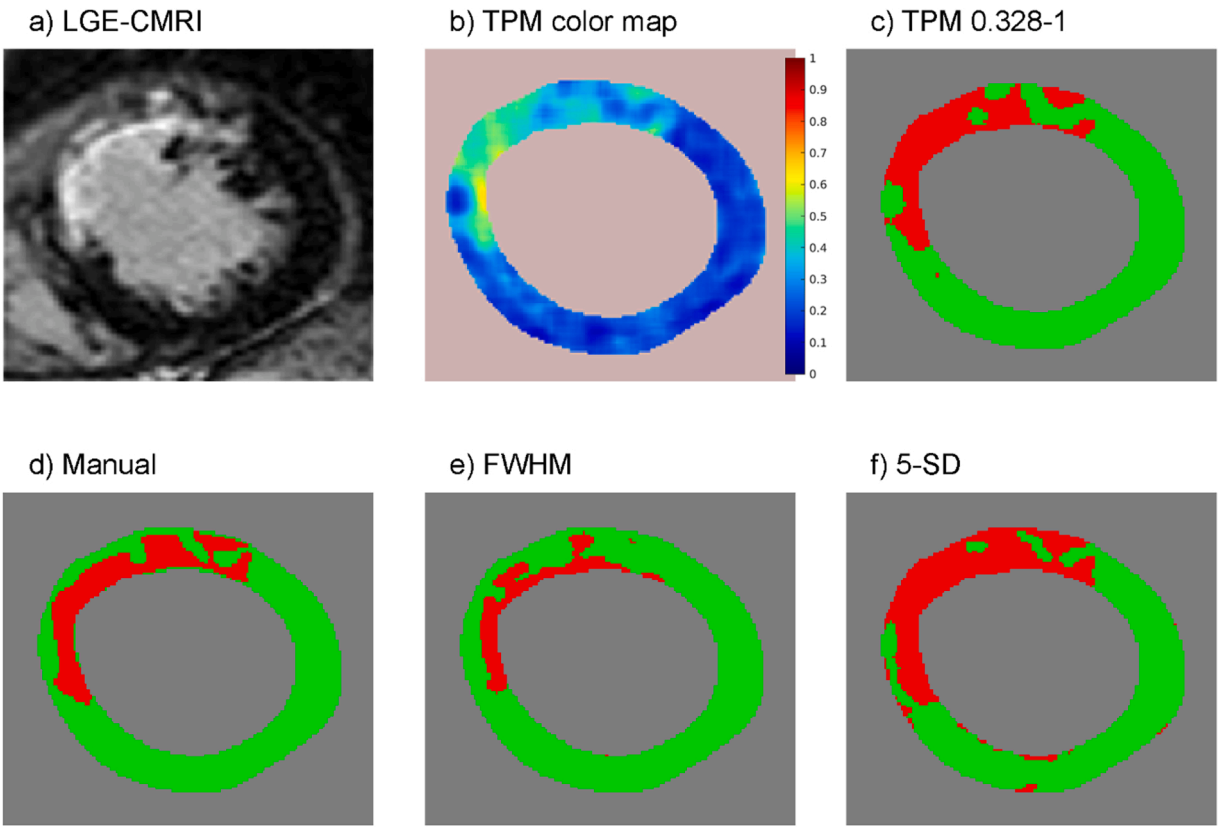

Fig. 4. Cross-sectional images of infarcted myocardium visualized by different methods a) Original cross sectional LGE-CMRI with Corresponding TPM color map without cutoff (b). Figure c-f illustrates the different scar delineation by using the four methods. Green and red colors indicate normal and scarred myocardium, respectively. The Scar is defined as pixels with probability mapping-values ≥ 0.328 (red), while pixels below this threshold are classified as normal myocardium (green).

Table 2
Infarct size estimated by the four methods.

Method	Scar size % of LV	Percentiles (25, 75)	*p* vs TPM	*p* vs Manual	*p* vs FWHM
TPM	23	(11, 32)	NA	99	002
Manual	19	(14, 26)	99	NA	01
FWHM	12	(8, 18)	002	001	NA
5-SD	26	(19, 33)	99	036	< 0.001

Scar size is presented as a percentage of the total number of pixels in the left ventricle (% of LV). Values are median and 25th and 75th percentiles. The p-values (adjusted by the Bonferroni correction for multiple tests) are calculated by independent-samples median test comparing the median infarct size between the four methods: Texture Probability Mapping, Manual delineation, Full Width Half Maximum (FWHM) and 5-standard deviation of remote myocardium (5-SD).

role for TPM in the assessment of myocardial fibrosis needs exploration in future studies.

There have been a growing number of publications on the topic radiomics and CMRI, especially with the focus on MI and myocarditis [15–17]. To our knowledge, there hasn't been any study presenting a probability mapping technique as a tool for the assessment of fibrosis comparable with our method. Fig. 6.

The TPM method is based upon dictionaries of textural information from LGE images from subjects with established myocardial scars [11]. The dictionaries have an impact on the output of the method. Both the core and the border zone of infarctions were included in the present scar tissue dictionary. The purpose of incorporating all parts of the ischemic scar in the present reference dictionary was to ensure that the method would recognize any type of myocardial scarring. Myocardial scars are heterogeneous, ranging from compact fibrous replacement tissue in the center of the scar to the border zone of the scar, being the transition between scarred and viable myocardium [18]. The diversity in tissue composition within a scar is a challenge when creating algorithms designed to identify scar tissue. Some scars are more compact, for example, in the case of transmural ST-elevation myocardial infarctions. Other scars are more diffuse, and infiltrative as seen in several cardiomyopathies [19,20]. The scars' border-zone and the development of diffuse myocardial fibrosis have been suggested to be related to the development of ventricular arrhythmias [21–23]. The identification and characterization of this type of fibrosis may aid the identification of subjects at risk of ventricular arrhythmias.

When comparing the TPM technique with the contemporary SI-based techniques for scar quantification, there are several important differences. Since the TPM method is based upon textural features, the method is not dependent on signal intensity as a reference value. Therefore, it is not necessary to find a ROI of the myocardium to calculate infarct size by the TPM method. This advantage reduces inter- and intraobserver variability and the time spent on analyzing LGE images.

The TPM method uses a dictionary including texture properties derived from the whole spectrum of infarcted myocardial tissue. In contrast, the FWHM primarily estimates the core of the infarction, whereas the 5-SD estimates the total infarction. It was, therefore as expected that the TPM method would estimate an infarct size between the 5-SD and the FWHM methods.

The n (5)-SD technique uses manual outlining of endocardial and epicardial borders and requires the delineation of a "normal" region (remote to the scar) to estimate the standard deviation (SD) of the reference SI. In the classic publication by Kim et al., a 2-SD of the SI of

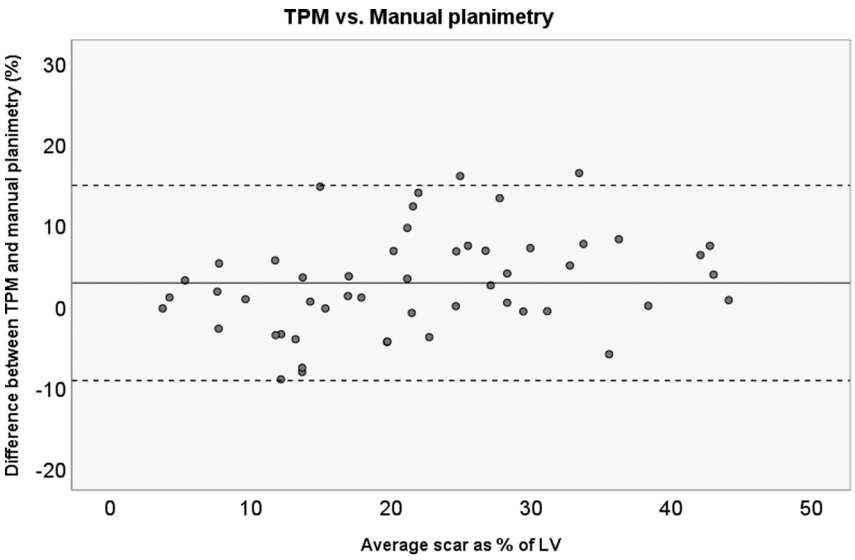

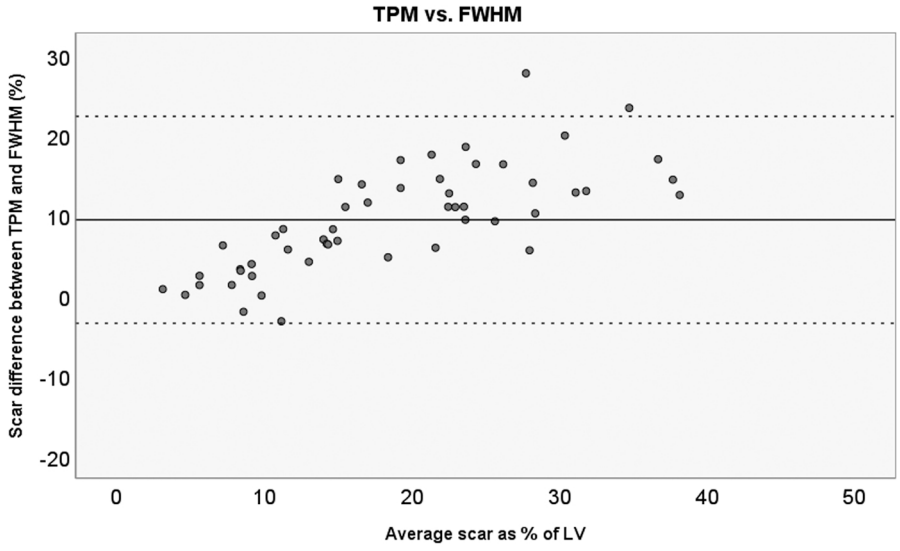

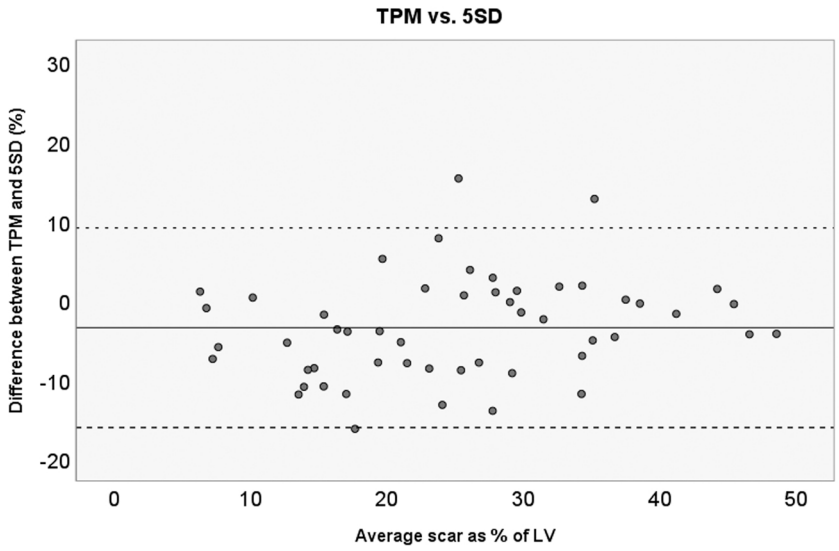

Fig. 5. a-c) Bland Altman plot of the TPM method compared with manual segmentation, FWHM and the 5 SD-technique. The Bland Altmann plots a-c show the agreement between the TPM-method and the SI-based techniques. The central line indicates the median difference, while the dotted lines represent the limits of agreement (median ± 1.96 x SD). With higher average scar size, the TPM method seems to estimate a higher scar size then FWHM. There is no significant difference between scar sizes estimated by the TPM method and the 5 SD-technique.

Table 3
Correlation coefficients (Spearman`s rho) between infarct size estimated by four different methods, and LVEF, LVEDVi and LVESVi.

Spearman`s rho	TPM	Manual	FWHM.	5-SD.
LVEF	-0.763*	-0.705*	-0.809*	-0.732*
LVEDVi	.727*	.715*	.792*	.736*
LVESVi	.751*	.717*	.817*	.743*

LVEF left ventricular ejection fraction, LVEDVi left ventricular end-diastolic volume index, LVESVi left ventricular end-systolic volume index.
* $p < 0.001$

the remote region was used to define the scar tissue [24]. Later studies showed that using 2-SD overestimates scar size [25,26]. Currently, 5-SD of remote SI is the recommended SD used to define scar size by this method [4]. However, as demonstrated by the present study, 5-SD still provides higher scar size estimates compared with the other methods [27]. Furthermore, the drawing of remote myocardium is susceptible to spatial variations in surface coil sensitivity [4]. To assess ischemic LGE, 5 standard deviations are recommended [4]. Even though the presence of LGE is automatically determined, it requires manual corrections to include areas with microvascular obstruction and to avoid areas with artifacts and blood pool in the left ventricle to be interpreted as infarction [4].

In line with other methods, the FWHM technique also requires manual segmentation of endocardial and epicardial borders. The method estimates infarct size by measuring all pixels above a threshold of 50% of the maximum intensity in the infarction in each slice [24,28]. The image is assessed visually, and if there is LGE present, the scar region containing maximum SI is manually selected. The FWHM technique is more reproducible than 5-SD [28]. As for the 5-SD technique, the FWHM technique is also vulnerable to spatial variations in surface coil sensitivity[29]. It could be more difficult to select the region with maximum SI in images with patchy or gray LGE, or several separate scars. In these patients, the method may be less accurate than the 5-SD method [4,24]. As mentioned for the 5-SD technique, manual correction is also necessary for no-reflow zones, artifacts and LV blood pool.

5. Limitations

The following study has several limitations: First, the study cohort is limited and only from a single center. Second, we are not in possession of animal models to verify our findings by histology. Our findings can therefore not be validated as representing true alterations in tissue characteristics. Third, the development of the TPM method started in 2010. The dictionaries in the program are based upon CMR images acquired prior to this date. The evaluation of the TPM method in the present study is therefore dependent upon the use of the same CMR methods, including the same contrast agent, the same hardware, the same settings, and the same software as used to generate the dictionaries. We, therefore, only included old images in the current study. The need to create new dictionaries for CMR examinations using other contrast agents and LGE protocols should be addressed by future studies. Fourth, we did not include a control group without pathological LGE. Fifth, we only included patients with infarct scar, and it is unclear whether the method will recognize fibrosis from other diseases such as midwall fibrosis in dilated cardiomyopathy, patchy fibrosis in hypertrophic cardiomyopathy or subepicardial fibrosis. This must be assessed in further studies.

Sixth, there are also limitations common for our method and current SI-methods. If parts of epicardial fat or intraventricular blood pool are

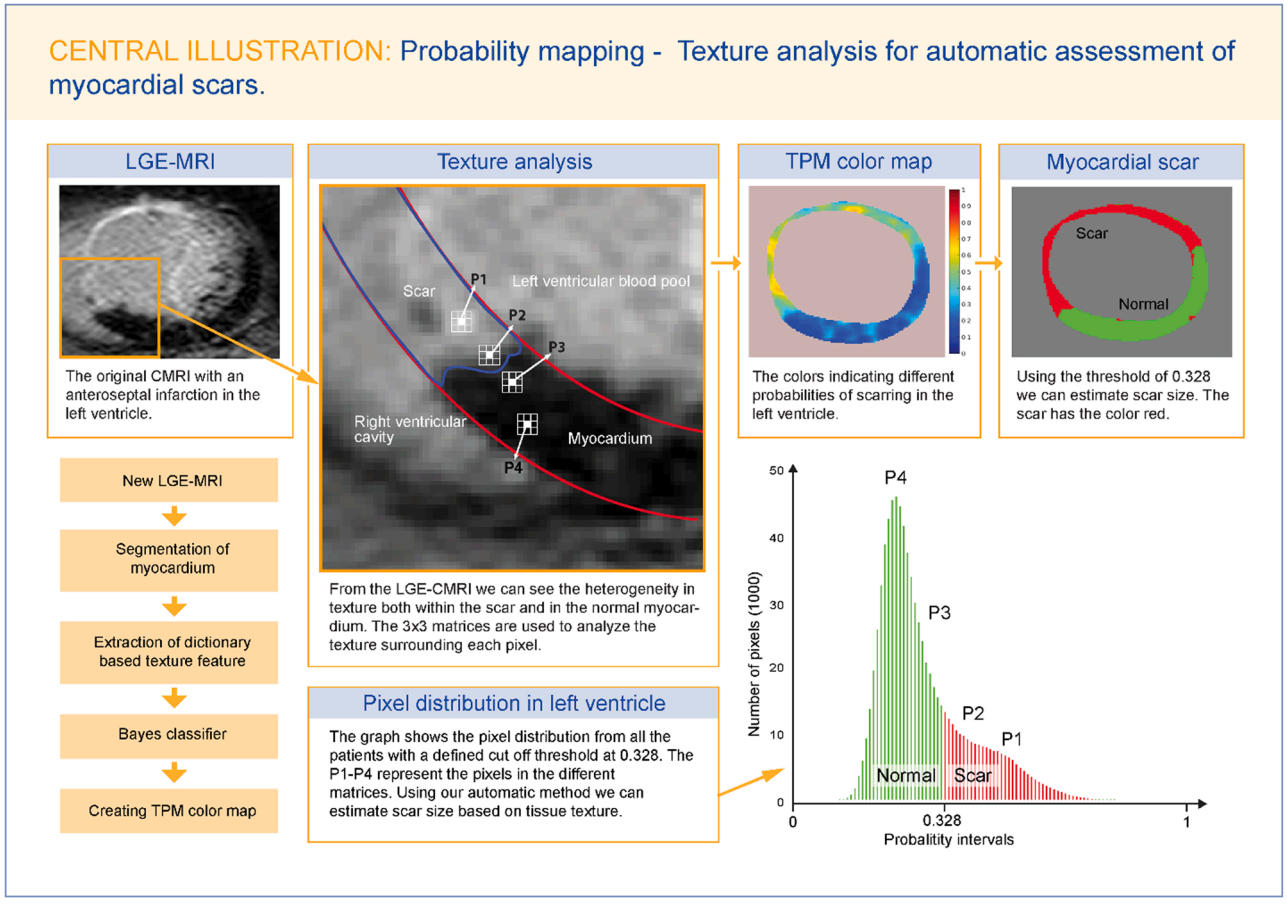

Fig. 6. Gives a summary of the creation of the TPM color map and highlights the selected probability range used to assess scar.

included, this may be misinterpreted by the TPM as scar tissue. Due to partial volume artifacts, there are challenges in the analysis of the most basal and apical cross-sectional image. If the inversion time does not null out the normal myocardium, it may cause overestimation of the infarction area. These problems are also relevant to current SI based methods.

Seventh, our study only includes patients with chronic scars, and the texture may be different in an acute MI. This is due to alternations in the underlying tissue composition in the acute phase of myocardial infarction. The acute phase consists of chaos of edema, microvascular obstruction (MO), inflammation and necrosis, which is later replaced with fibrosis [18]. The present TPM method has been programmed to recognize the characteristics of MO. However, our study only contains LGE images from patients with old scars. Future studies need to evaluate TPM in the early phase following acute myocardial infarction.

6. Conclusion

TPM is comparable to the conventional SI-based method for quantification of scar burden following MI. Scar size assessed by TPM shows strong correlations with left ventricular remodeling parameters.

Ethical statement

The analysis was approved by The Regional Ethics Committee (REK Vest: 3.2005.1312). All included patients signed an informed consent.

Funding

This work was supported by a PhD scholarship grant from the Western Norway Regional Health Authority, grant ID 912296.

Declaration of Competing Interest

The authors declare that they have no known competing financial interests or personal relationships that could have appeared to influence the work reported in this paper.

Acknowledgments

The authors wish to thank Roald Tungland for his important contributions in the study.

References

[1] S. Orn, C. Manhenke, O.J. Greve, A.I. Larsen, V.V. Bonarjee, T. Edvardsen, K. Dickstein, Microvascular obstruction is a major determinant of infarct healing and subsequent left ventricular remodelling following primary percutaneous coronary intervention, Eur. Heart J. 30 (16) (2009) 1978–1985.
[2] D.C. Lee, J.J. Goldberger, CMR for sudden cardiac death risk stratification: are we there yet? JACC Cardiovasc. Imaging 6 (3) (2013) 345–348.
[3] N. Mewton, C.Y. Liu, P. Croisille, D. Bluemke, J.A. Lima, Assessment of myocardial fibrosis with cardiovascular magnetic resonance, J. Am. Coll. Cardiol. 57 (8) (2011) 891–903.
[4] J. Schulz-Menger, D.A. Bluemke, J. Bremerich, S.D. Flamm, M.A. Fogel, M. G. Friedrich, R.J. Kim, F. von Knobelsdorff-Brenkenhoff, C.M. Kramer, D.J. Pennell, S. Plein, E. Nagel, Standardized image interpretation and post-processing in cardiovascular magnetic resonance - 2020 update: society for cardiovascular magnetic resonance (SCMR): board of trustees task force on standardized post-processing, J. Cardiovasc. Magn. Reson. 22 (1) (2020) 19.
[5] C. Hassani, F. Saremi, B.A. Varghese, V. Duddalwar, Myocardial radiomics in cardiac MRI, Am. J. Roentgenol. 214 (3) (2019) 536–545.
[6] C. Hassani, B.A. Varghese, J. Nieva, V. Duddalwar, Radiomics in pulmonary lesion imaging, Am. J. Roentgenol. 212 (3) (2019) 497–504.
[7] L.Y. Hsu, A. Natanzon, P. Kellman, G.A. Hirsch, A.H. Aletras, A.E. Arai, Quantitative myocardial infarction on delayed enhancement MRI. Part I: animal validation of an automated feature analysis and combined thresholding infarct sizing algorithm, J. Magn. Reson. Imaging 23 (3) (2006) 298–308.
[8] B.A. Varghese, S.Y. Cen, D.H. Hwang, V.A. Duddalwar, Texture analysis of imaging: what radiologists need to know, Am. J. Roentgenol. 212 (3) (2019) 520–528.
[9] A. Larroza, V. Bodí, D. Moratal, Texture analysis in magnetic resonance imaging: review and considerations for future applications, in: C. Constantinides (Ed.), Assessment of Cellular and Organ Function and Dysfunction using Direct and Derived MRI Methodologies, IntechOpen, 2016, pp. 75–106.
[10] A. Kassner, R.E. Thornhill, Texture analysis: a review of neurologic MR imaging applications, AJNR Am. J. Neuroradiol. 31 (5) (2010) 809–816.
[11] L.P. Kotu, K. Engan, K. Skretting, F. Maloy, S. Orn, L. Woie, T. Eftestol, Probability mapping of scarred myocardium using texture and intensity features in CMR images, Biomed. Eng. Online 12 (2013) 91.
[12] L. Woie, T. Eftestol, K. Engan, J.T. Kvaloy, D.W. Nilsen, S. Orn, The heart rate of ventricular tachycardia following an old myocardial infarction is inversely related to the size of scarring, Europace 13 (6) (2011) 864–868.
[13] L.R. Dice, Measures of the amount of ecologic association between species, Ecol. Evol. (1945) 297–302.
[14] T. Sørensen, A method of establishing groups of equal amplitude in plant sociology based on similarity of species and its application to analyses of the vegetation on Danish commons, Biologiske Skrifter 4 (1948).
[15] B. Baessler, C. Luecke, J. Lurz, K. Klingel, M. von Roeder, S. de Waha, C. Besler, D. Maintz, M. Gutberlet, H. Thiele, P. Lurz, Cardiac MRI texture analysis of T1 and T2 maps in patients with infarctlike acute myocarditis, Radiology 289 (2) (2018) 357–365.
[16] T. Di Noto, J. von Spiczak, M. Mannil, E. Gantert, P. Soda, R. Manka, H. Alkadhi, Radiomics for distinguishing myocardial infarction from myocarditis at late gadolinium enhancement at MRI: comparison with subjective visual, Anal., Radiol. Cardiothorac. Imaging 1 (5) (2019), e180026.
[17] A. Larroza, M.P. Lopez-Lereu, J.V. Monmeneu, J. Gavara, F.J. Chorro, V. Bodi, D. Moratal, Texture analysis of cardiac cine magnetic resonance imaging to detect nonviable segments in patients with chronic myocardial infarction, Med. Phys. 45 (4) (2018) 1471–1480.
[18] V. Talman, H. Ruskoaho, Cardiac fibrosis in myocardial infarction-from repair and remodeling to regeneration, Cell Tissue Res. 365 (3) (2016) 563–581.
[19] S.J. Park, S.W. Cho, S.M. Kim, J. Ahn, K. Carriere, D.S. Jeong, S.C. Lee, S.W. Park, Y.H. Choe, P.W. Park, J.K. Oh, Assessment of myocardial fibrosis using multimodality imaging in severe aortic stenosis: comparison with histologic fibrosis, JACC Cardiovasc. Imaging 12 (1) (2019) 109–119.
[20] F. aus dem Siepen, S.J. Buss, D. Messroghli, F. Andre, D. Lossnitzer, S. Seitz, M. Keller, P.A. Schnabel, E. Giannitsis, G. Korosoglou, H.A. Katus, H. Steen, T1 mapping in dilated cardiomyopathy with cardiac magnetic resonance: quantification of diffuse myocardial fibrosis and comparison with endomyocardial biopsy, Eur. Heart J. Cardiovasc. Imaging 16 (2) (2015) 210–216.
[21] O.A. Ajijola, R. Tung, K. Shivkumar, Ventricular tachycardia in ischemic heart disease substrates, Indian Heart J. 66 (Suppl 1) (2014) S24–S34.
[22] H.H. Hsia, D. Lin, W.H. Sauer, D.J. Callans, F.E. Marchlinski, Anatomic characterization of endocardial substrate for hemodynamically stable reentrant ventricular tachycardia: identification of endocardial conducting channels, Heart Rhythm 3 (5) (2006) 503–512.
[23] A. Verma, N.F. Marrouche, R.A. Schweikert, W. Saliba, O. Wazni, J. Cummings, A. Abdul-Karim, M. Bhargava, J.D. Burkhardt, F. Kilicaslan, D.O. Martin, A. Natale, Relationship between successful ablation sites and the scar border zone defined by substrate mapping for ventricular tachycardia post-myocardial infarction, J. Cardiovasc. Electrophysiol. 16 (5) (2005) 465–471.
[24] H.W. Kim, A. Farzaneh-Far, R.J. Kim, Cardiovascular magnetic resonance in patients with myocardial infarction: current and emerging applications, J. Am. Coll. Cardiol. 55 (1) (2009) 1–16.
[25] R.Y. Kwong, A. Farzaneh-Far, Measuring myocardial scar by CMR, JACC Cardiovasc. Imaging 4 (2) (2011) 157–160.
[26] D. Corcoran, C. Berry, How to measure myocardial infarct size by cardiac magnetic resonance imaging, Heart Metab. 70 (2016) 14–18.
[27] J.N. Khan, S.A. Nazir, M.A. Horsfield, A. Singh, P. Kanagala, J.P. Greenwood, A. H. Gershlick, G.P. McCann, Comparison of semi-automated methods to quantify infarct size and area at risk by cardiovascular magnetic resonance imaging at 1.5T and 3.0T field strengths, BMC Res. Notes 8 (2015) 52.
[28] A.S. Flett, J. Hasleton, C. Cook, D. Hausenloy, G. Quarta, C. Ariti, V. Muthurangu, J.C. Moon, Evaluation of techniques for the quantification of myocardial scar of differing etiology using cardiac magnetic resonance, JACC Cardiovasc. Imaging 4 (2) (2011) 150–156.
[29] L.C. Amado, B.L. Gerber, S.N. Gupta, D.W. Rettmann, G. Szarf, R. Schock, K. Nasir, D.L. Kraitchman, J.A. Lima, Accurate and objective infarct sizing by contrast-enhanced magnetic resonance imaging in a canine myocardial infarction model, J. Am. Coll. Cardiol. 44 (12) (2004) 2383–2389.